Supporting Information

Synthesis of Lanthanide-based scintillator@MOF nanocomposites for X-ray-induced photodynamic therapy

Lantian Zhang[a], Fan Gao[a], Shiqi Liu[a], Mei Ju[c], Chao Sun[d] Gengzhi Sun[a], Qiang Ju*[a], Kai Yang*[b], Zhenlan Fang*[a]

[a]Key Laboratory of Flexible Electronics (KLOFE) & Institute of Advanced Materials (IAM), Jiangsu National Synergetic Innovation Center for Advanced Materials (SICAM), Nanjing Tech University (NanjingTech), Nanjing, 211816, P.R. China. Email: iamqju@njtech.edu.cn

[b]State Key Laboratory of Radiation Medicine and Protection, School of Radiation Medicine and Protection and School for Radiological and Interdisciplinary Sciences (RAD-X), Collaborative Innovation Center of Radiation Medicine of Jiangsu Higher Education Institutions, Soochow University, Suzhou, 215123, P.R. China. Email: kyang@suda.edu.cn

[c]Hospital for Skin Disease, Institute of Dermatology, Chinese Academy of Medical Sciences & Peking Union Medical College, Nanjing, 210042, China.

[d]Department of Urology, Zhongda Hospital affiliated to Southeast University, Nanjing, 210096, China.

X-ray induced ROS generation

ROS generation was examined by photo-degradation of DPBF. In this assay, SNPs (500 μg mL^{-1}), SNPs@Hf-TCPP (500 μg mL^{-1}) aqueous solution and blank group (H_2O) were firstly mixed with 50 μM DPBF/DMSO solution. Then, the mixture was irradiated with X-ray of 0, 2, 4, 6, 8, and 10 Gy using a dose rate of 1.226 Gy min^{-1}. Finally, the absorbance spectra of solution were immediately monitored with UV/vis spectroscopy, and the intensity of absorption band centered as 410 nm was calculated.

X-ray induced $^1O_2$ generation

SOSG was applied to detect the generation of $^1O_2$, which can induce the emission of SOSG at 525 nm. Specifically, SNPs (500 μg mL^{-1}), and SNPs@Hf-TCPP (500 μg mL^{-1}) aqueous solution and blank group (H_2O) were mixed with 100 μM SOSG methanol solution. Then, the mixture was irradiated with X-ray of 0, 2, 4, 6, 8, and 10 Gy using a dose rate of 1.226 Gy min^{-1}. Finally, the fluorescence intensity of SOSG was measured upon excitation at 488 nm.

X-ray induced •OH generation

•OH was detected by TMB as the trapping agent with the characteristic absorption peak at 652 nm. SNPs (500 μg mL^{-1}), and SNPs@Hf-TCPP (500 μg mL^{-1}) aqueous solution and blank group (H_2O) were firstly mixed with 200 μM TMB/DMSO solution, and then, the mixture was irradiated with X-ray of 0, 2, 4, 6, 8, and 10 Gy using a dose rate of 1.226 Gy min^{-1}. After X-ray treatment, the absorption spectra of solutions were immediately measured by UV/vis spectroscopy.

Synthesis of SNPs@Hf-TCPP-PEG nanocomposites.

50 mg as-prepared SNPs@Hf-TCPP nanocomposites dispersed in 5 mL H_2O was introduced to 10 mL H_2O containing 1-(3-Dimethylaminopropyl)-3-ethylcarbodiimide hydrochloride (EDC,100 mg). The mixture was stirred for 30 minutes at room temperature, followed by the addition of 75 mg methoxypolyethylene glycol amine (PEG) and stirring for 12 hours. The product SNPs@Hf-TCPP-PEG was collected by

centrifugation and washed with H_2O for three times.

Cell viability study by MTT assay

The 4T1 cell lines were originally obtained from American Type Culture Collection (ATCC). Cells were grown in normal RPMI-1640 culture medium with 10% fetal bovine serum (FBS) and 1% penicillin/streptomycin. The cells pre-seeded into 96 well cell culture plates at 2×10^5 cells/well were incubated with different concentrations of SNPs and SNPs@Hf-TCPP nanocomposites (all the samples are PEGylated in the following cell experiments) for 24 h followed by X-ray irradiation (2 Gy), and the standard (MTT) assay was carried out to determine the cell viabilities. The each well plate was treated with 10 μL of freshly prepared MTT solution (5 mg mL^{-1} in PBS buffer of pH 7.4) and incubated for 4 h. The supernatant was carefully removed leaving behind the violet formazon crystals in the plate. The crystals dissolved in DMSO were recorded at 450 nm using a microplate reader.

Cellular uptake of nanocomposites

The cellular uptake of SNPs@Hf-TCPP nanocomposites was examined on GL216 cells. The cells were placed in culture dish with a glass bottom at 1×10^5 cells per well. After adhesion, the nanocomposites (50 μg/mL) were added into wells and cultured for 3 h. After washing with PBS (pH 7.4) for three times, the cells were fixed and subsequently stained with 4,6-diamidino-2-phenylindole (DAPI), followed by imaging using a laser scanning confocal microscope (Ti C2+, Nikon Corporation, Japan).

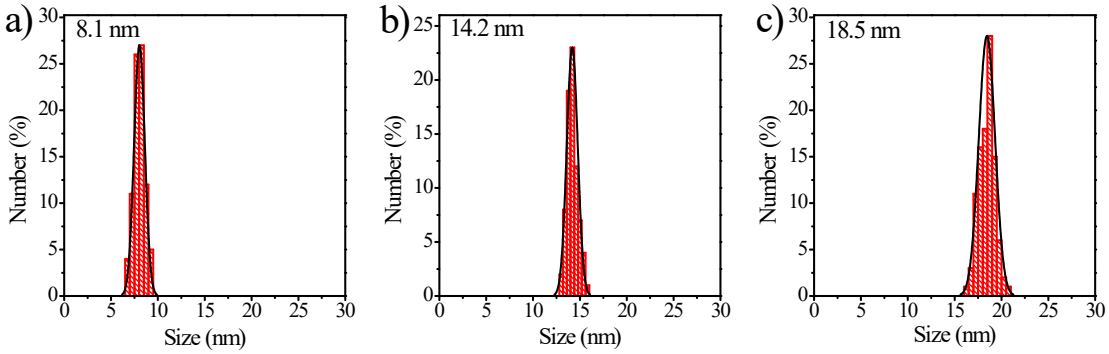

Figure S1. Size distributions of (a) $NaGdF_4$: 30 at.% Tb, (b) $NaGdF_4$: 30 at.% Tb@$NaGdF_4$: 20 at.% Ce and (c) $NaGdF_4$: 30 at.% Tb@$NaGdF_4$: 20 at.% Ce @$NaLuF_4$ nanoparticles obtained from their corresponding TEM images.

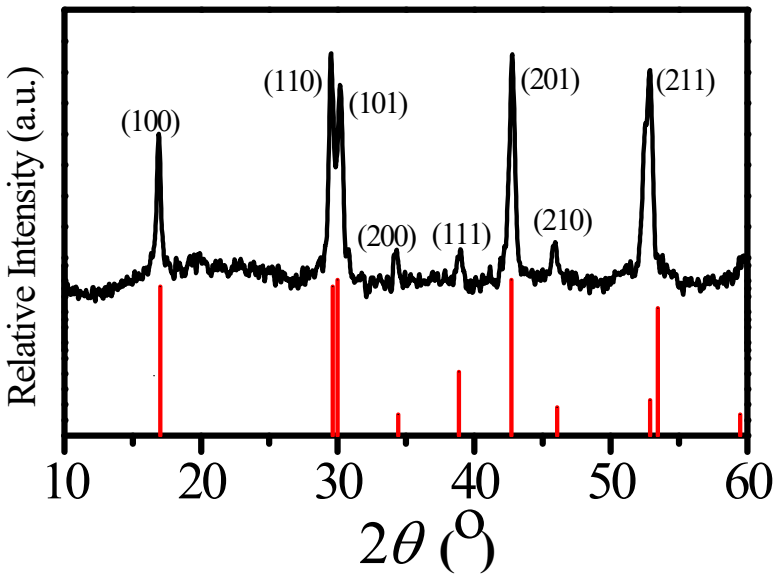

Figure S2. XRD pattern (black) of $NaGdF_4$: Tb@$NaGdF_4$: Ce @$NaLuF_4$ SNPs, and the standard card (red) of hexagonal-phase $NaGdF_4$ (JCPDS no.27-0699).

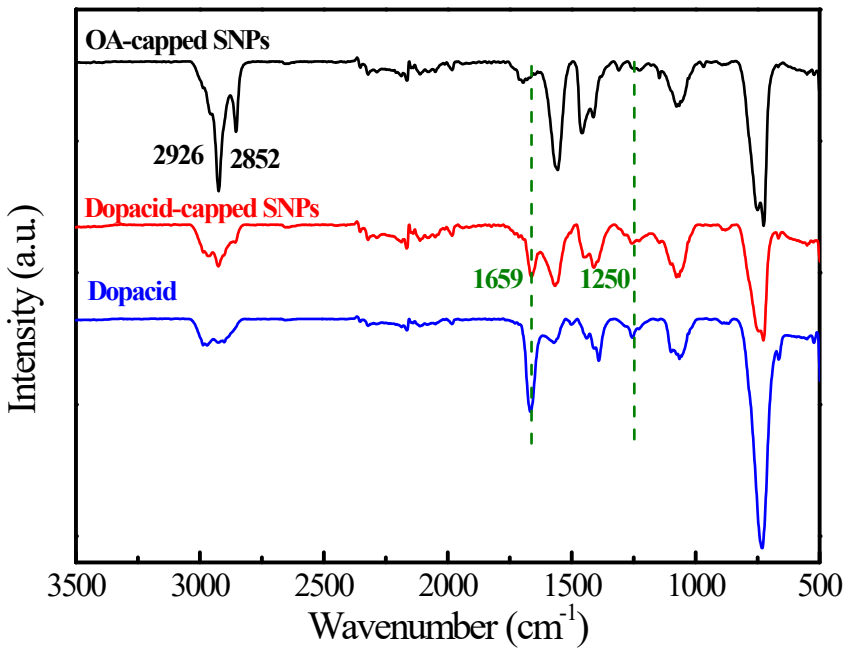

Figure S3. FTIR spectra of SNPs before and after ligand exchange. Original OA-capped SNPs show strong bands peaked at 2926 and 2852 cm^{-1}, assigned to the stretching and rocking vibration of -CH_2- in OA. After ligand exchange, the stretching vibrations of C=O and C-O located at 1659 and 1250 cm^{-1} are observed, which can also be detected in Dopacid, while the -CH_2- peaks significantly decrease, indicating that Dopacid successfully substitutes OA and coats on the surface of SNPs.

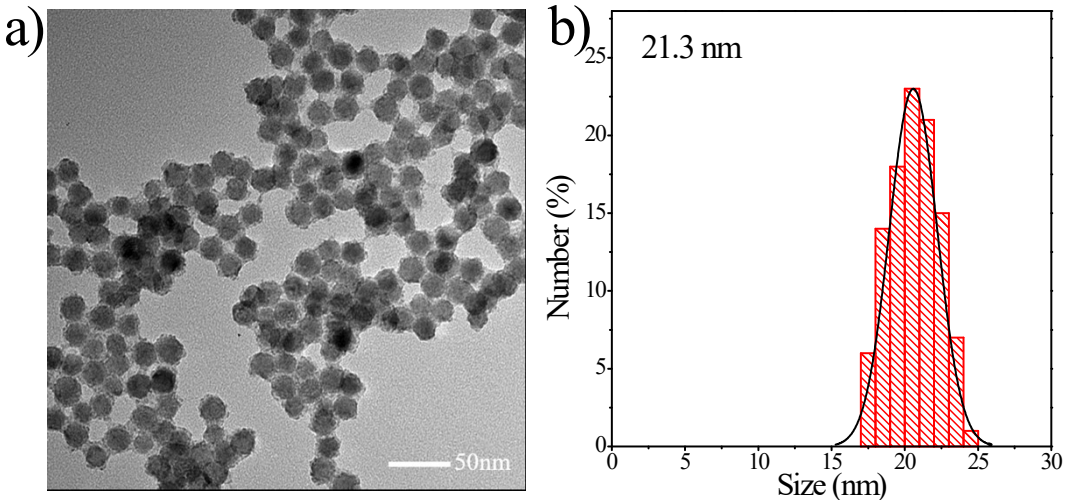

Figure S4. (a) TEM image and (b) the corresponding particle size distribution of the SNPs@Hf-TCPP nanocomposites.

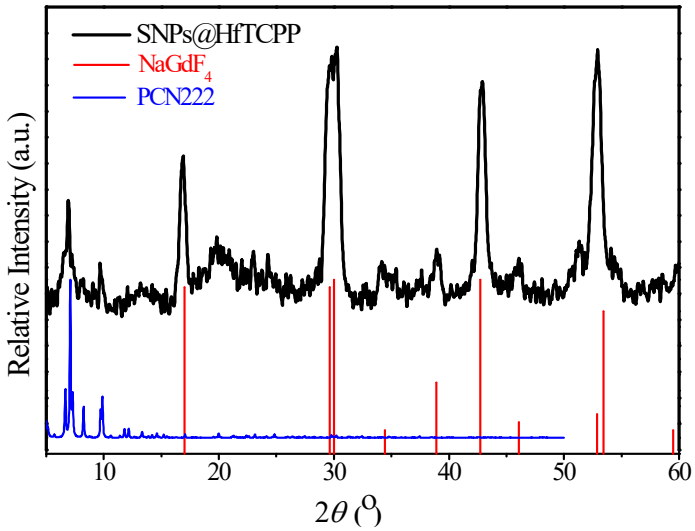

Figure S5. XRD pattern of SNPs@Hf-TCPP nanocomposites. The line patterns of SNPs are hexagonal-phase $NaGdF_4$ (JCPDS standard card no. 27-0699), and Hf-TCPP adopted hexagonal PCN-222 structure (PCN refers to porous coordination networks) according to the literature (*Angew. Chem., Int. Ed.* 2012, *51*, 10307). SNPs@Hf-TCPP can be clearly identified as consisting of hexagonal-phase $NaGdF_4$ and hexagonal PCN-222 without the presence of other impurities.

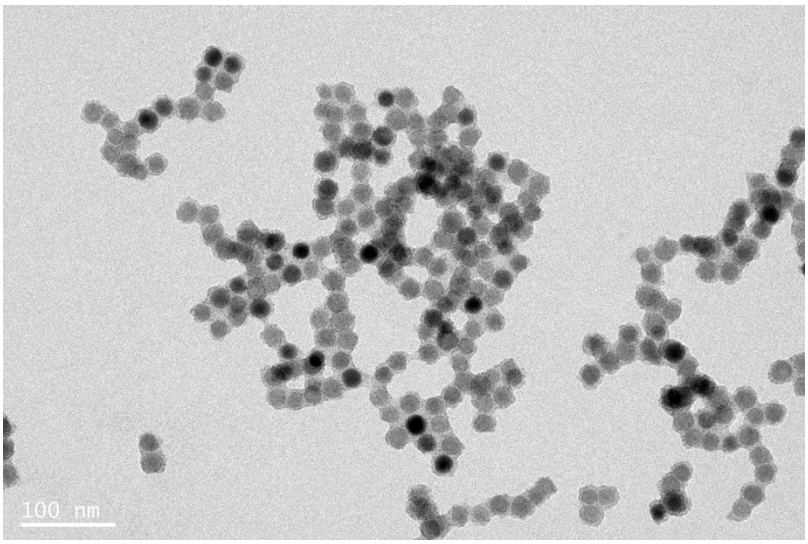

Figure S6. TEM image of SNPs@Hf-TCPP nanocomposites dispersed in water for 7 months. This result exhibits a well-organized core-shell structure and indicated a stability in aqueous solution.

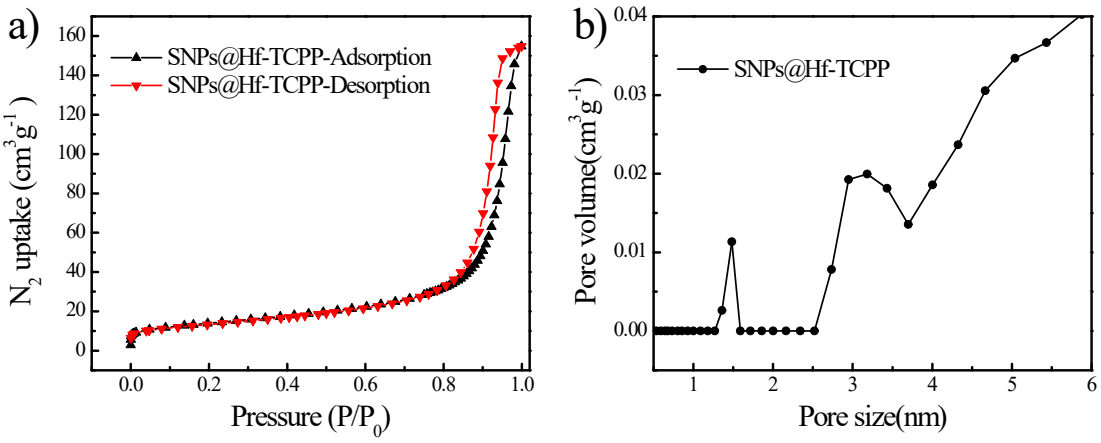

Figure S7. (a) N_2 adsorption-desorption isotherms and (b) pore size distributions of SNPs@Hf-TCPP nanocomposites, exhibiting a typical type IV adsorption N_2 isotherm with mesoporous structure characteristics.

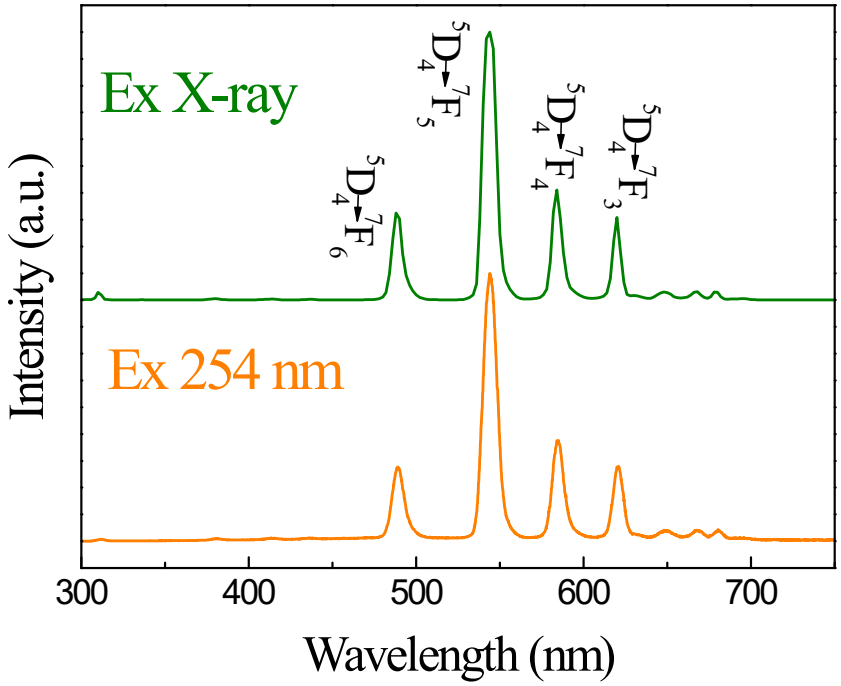

Figure S8. Emission spectra of OA-capped SNPs under the excitation of X-ray and 254 nm, respectively. The SNPs demonstrates the similar emission spectra under different excitation/irradiation.

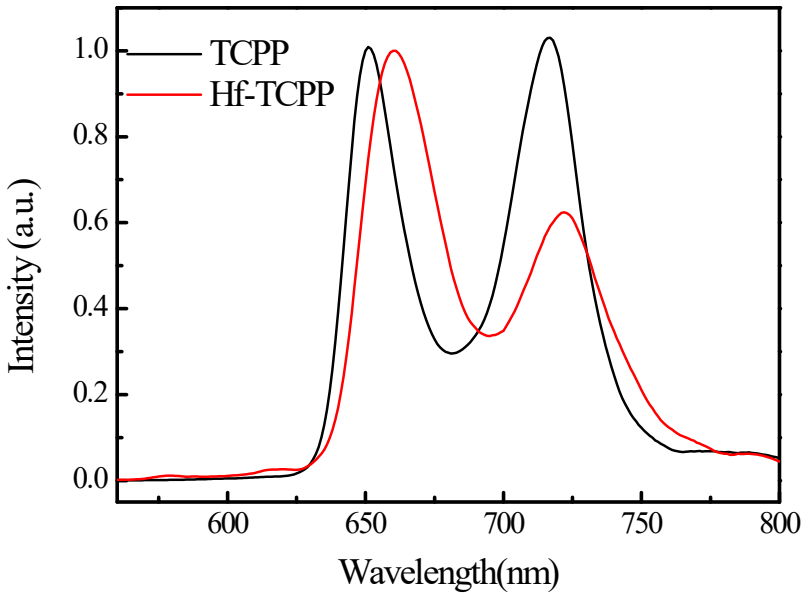

Figure S9. The emission spectra of monomeric TCPP and Hf-TCPP under the excitation of 420 nm. The monomeric TCPP are located at 651 nm and 716 nm, while the emission peaks for Hf-TCPP are located at 660 nm and 722 nm. The red shift of the emission peaks in Hf-TCPP is attributed to the strong coupling of excitonic states due to the short intermolecular distance in such highly compact and ordered TCPP networks (*Nano Lett.* 2021, 21, 2, 1102–1107).

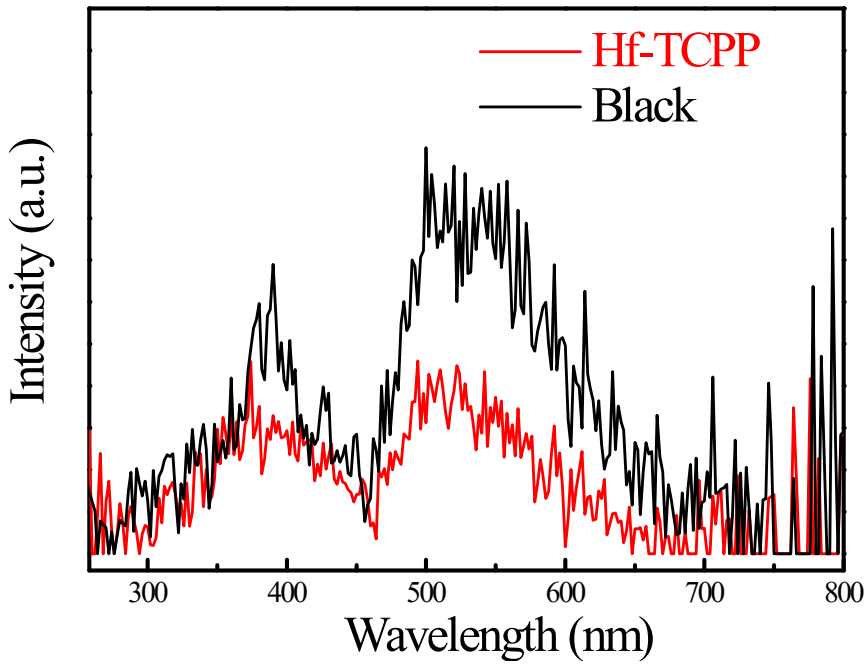

Figure S10. Emission spectra of Hf-TCPP (red) and the blank experiment (black) under the excitation of X-ray, indicating that there is no emission of Hf-TCPP under X-ray irradiation.

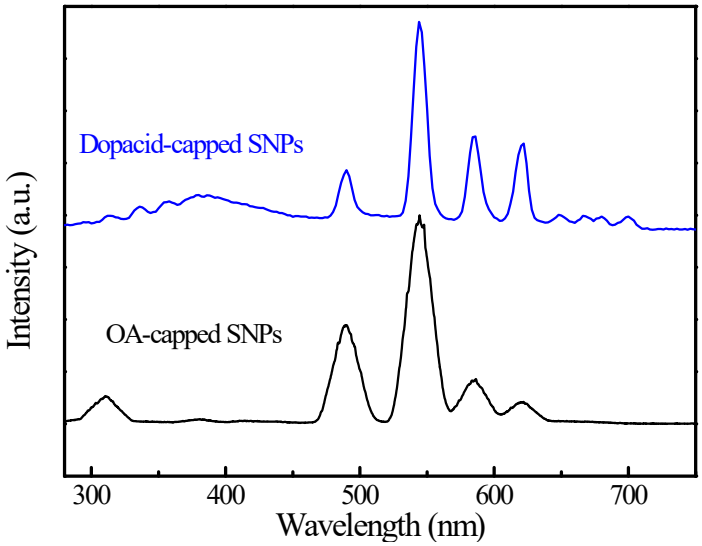

Figure S11. Emission spectra of Dopacid-capped SNPs and OA-capped SNPs under the excitation of X-ray, respectively. After Dopacid substituting OA, the broad band centered at 385 nm was presented, indicating that this emission band originates from the surface-capped Dopacid.

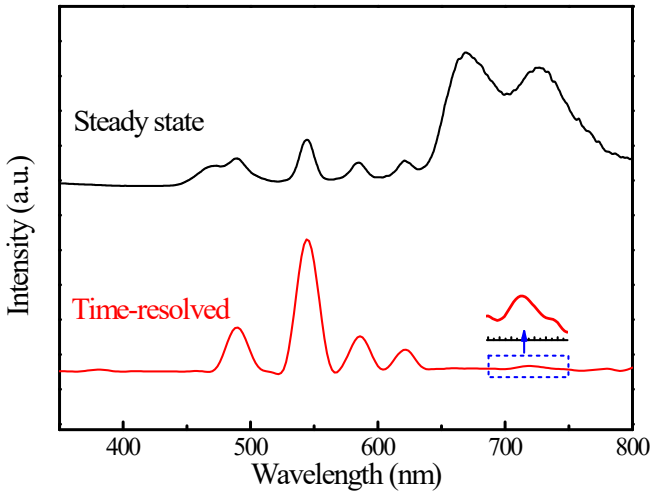

Figure S12. Steady state and time-resolved spectra (delay time = 20 μs, gate time = 1 ms) of nanocomposites under the excitation of 254 nm. TCPP emission band is strong in steady-state spectra, but weak in time-resolved spectra because its intrinsic lifetime (<10 ns) is much shorter than the delay time. In contrast to the weak emission of TCPP in time-resolved spectra, which is realized by the resonant energy transfer from long-lived Tb^{3+}, the strong emission of TCPP in XEF (Figure 3e) should mainly be achieved by the reabsorption of Tb^{3+}.

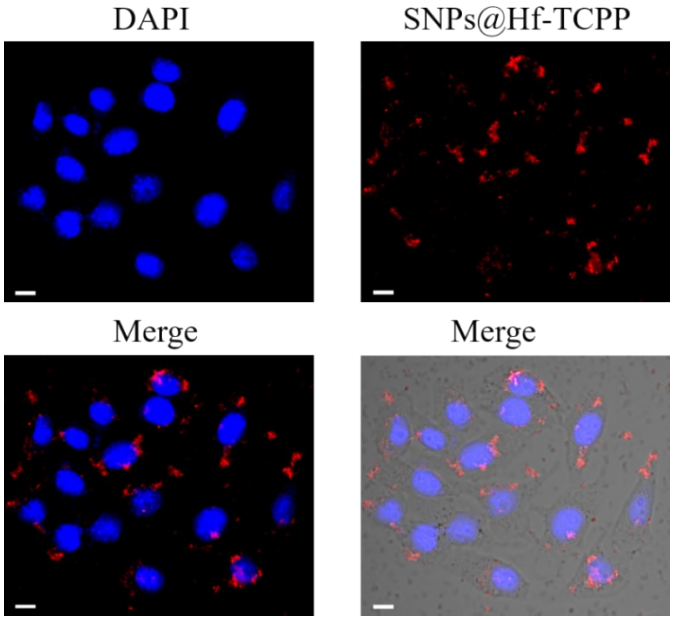

Figure S13. Confocal fluorescence images of GL216 cells incubated with SNPs@Hf-TCPP nanocomposites for 3 h, scale bar is 10 μm. Blue fluorescence indicates nucleus from DAPI and red fluorescence is attributed to TCPP. The red fluorescence signal belonging to TCPP can be significantly observed, indicating efficient cellular internalization of SNPs@Hf-TCPP nanocomposites.